

## Shear Flow of Non-Brownian Suspensions Close to Jamming

Bruno Andreotti,<sup>1</sup> Jean-Louis Barrat,<sup>2</sup> and Claus Heussinger<sup>3,4</sup>

<sup>1</sup>*Physique et Mécanique des Milieux Hétérogènes, UMR 7636 ESPCI -CNRS, Univ. Paris-Diderot, 10 rue Vauquelin, 75005, Paris*

<sup>2</sup>*LIPHY, Univ. Grenoble 1; UMR 5588 et CNRS, F-38402 Saint Martin d'Hères, France*

<sup>3</sup>*Institute for Theoretical Physics, Georg-August University of Göttingen, Friedrich-Hund Platz 1, 37077 Göttingen, Germany*

<sup>4</sup>*Max Planck Institute for Dynamics and Self-Organization, Am Faßberg 17, 37077 Göttingen, Germany*

(Received 14 December 2011; published 6 September 2012)

The dynamical mechanisms controlling the rheology of dense suspensions close to jamming are investigated numerically, using simplified models for the relevant dissipative forces. We show that the velocity fluctuations control the dissipation rate and therefore the effective viscosity of the suspension. These fluctuations are similar in quasi-static simulations and for finite strain rate calculations with various damping schemes. We conclude that the statistical properties of grain trajectories—in particular the critical exponent of velocity fluctuations with respect to volume fraction  $\phi$ —only weakly depend on the dissipation mechanism. Rather they are determined by steric effects, which are the main driving forces in the quasistatic simulations. The critical exponent of the suspension viscosity with respect to  $\phi$  can then be deduced, and is consistent with experimental data.

DOI: [10.1103/PhysRevLett.109.105901](https://doi.org/10.1103/PhysRevLett.109.105901)

PACS numbers: 83.80.Hj, 66.20.Cy

Athermal disordered systems such as foams [1], emulsions [2], nonBrownian suspensions [3], or granular materials [4] exhibit a critical phase transition between liquid-like and solid-like mechanical behavior when the particle volume fraction  $\phi$  crosses the jamming point  $\phi_c$ . For  $\phi > \phi_c$ , these amorphous systems can resist shear. The elastic shear modulus vanishes at  $\phi_c$  with a critical exponent different from the mean field one [5,6]. Above the yield stress  $\sigma_Y$ , vanishing at  $\phi_c$ , they present a nonNewtonian rheology, for which several different interpretations based on (i) an analogy with the glassy dynamics of a system presenting scale-free energy distributions [7], (ii) interacting plastic events [8], and (iii) the critical scaling laws of the shear modulus and coordination number [9] have been proposed. Together with the conventional molecular dynamic (MD) simulations, quasistatic (QS) methods have been applied to study the plastic flow of athermal amorphous solids at the yield-stress  $\sigma_Y$  [10–14] level. It is generally assumed that QS methods accurately describe the dynamics of the true system in the limit of asymptotically small shear rate  $\dot{\gamma}$ . However, the existence of a proper QS limit remains controversial, and there is growing evidence that QS flows actually correspond to a finite-size dominated regime, with a correlation length that saturates at the system size [8,14].

Symmetrically, for  $\phi < \phi_c$ , amorphous materials can flow under an infinitesimal shear stress  $\sigma$  and present a viscosity  $\eta$  diverging at  $\phi_c$ , like  $\eta \propto (\phi_c - \phi)^{-\alpha}$ . Scaling laws are expected to be different in thermal (glassy) and athermal systems [15]. In the case of a suspension of nonBrownian particles, the best fit of recent experimental results give a critical exponent of  $\alpha = 2.4$  for volume-controlled experiments [16] and of  $\alpha = 1.9$  for pressure-controlled experiments [3]. The explanations of the critical

exponent as well as the underlying mechanisms of the flow arrest have remained open and controversial questions up to now. Among the proposed mechanisms is the hydrodynamic dissipation in lubricated films separating the particles, or friction-induced normal stresses [17]. A completely different interpretation relates the divergence of the viscosity to a singular mode of the network of contacts close to the isostatic point [18].

Here, we present simulation results for the viscous flow of a simplified model system in the vicinity of the close-packed state at  $\phi_c$ . We identify a dynamical contribution to the divergence of the viscosity, which has its origin in the singularity of velocity fluctuations. By comparing different computational model systems, we show that some of the statistical properties of these velocity fluctuations are surprisingly model independent. We show how the rheological properties, in particular the form of the flow curve and divergence of the viscosity, can be obtained from one set of trajectories based on a QS simulation method.

*Simulations.*—We consider a two-dimensional system constituted by  $N$  soft spherical particles of mass  $m$ ,  $N/2$  of diameter  $d$ , and  $N/2$  of diameter  $1.4d$ . The particle volume fraction is defined as  $\phi = \sum_{i=1}^N \pi r_i^2 / L^2$ , where  $L$  is the size of the simulation box. Periodic (Lees-Edwards) boundary conditions are used in both directions. Two particles  $i, j$  interact when their distance  $r$  is smaller than the sum of their radii,  $r_i + r_j$ , with a repulsive potential  $E(r) = \epsilon(1 - r/(r_i + r_j))^2$ . All the observables below are given in units of  $d$ ,  $m$ , and  $\epsilon$ . We compare the divergence of the viscosity for  $\phi < \phi_c = 0.843$  [13,19] using two different dynamics: nonequilibrium dissipative MD and QC simulations.

In MD simulations, the system is sheared at a shear rate  $\dot{\gamma}$ . Newton's equations of motion  $m\ddot{\vec{r}}_i = \vec{F}_i^{\text{el}} + \vec{F}_i^{\text{visc}}$  are

integrated with elastic contact forces  $\vec{F}^{\text{el}} = -\vec{\nabla}E$  and a viscous drag force

$$\vec{F}^{\text{visc}}(\vec{v}_i) = -\zeta \delta \vec{v}_i |\delta \vec{v}_i|^{\nu-1}, \quad (1)$$

proportional to the  $\nu$ th power of the velocity difference  $\delta \vec{v}_i = \vec{v}_i - \vec{v}_{\text{flow}}$  between the particle velocity  $\vec{v}_i$  and the flow velocity  $\vec{v}_{\text{flow}}(\vec{r}_i) = \vec{e}_x \dot{\gamma} y$ , whose fluctuations are ignored [20–23]. The flow can be viewed as being set up by a nonNewtonian fluid characterized by a friction coefficient  $\zeta$ . In the special case  $\nu = 1$ , the fluid is Newtonian and  $\zeta$  is proportional to the bare fluid viscosity  $\eta_f$  (in Stokes approximation,  $\zeta = 3\pi\eta_f d$ ). Thermal and lubrication forces are ignored. Unlike in granular systems, the particle-particle collisions are elastic and the only dissipation is due to viscous losses associated with the fluctuations of the particle velocity field. The shear stress  $\sigma$  is calculated from the particle positions  $\vec{r}_i = (x_i, y_i)$  and the forces  $\vec{F}_i = (F_{ix}, F_{iy})$  acting on them as  $\sigma = L^{-2} \sum_{i=1}^N x_i F_{iy}$ . The dominant contribution comes from the elastic forces that result from particle overlaps. The resulting relation between the shear stress  $\sigma$  and shear rate  $\dot{\gamma}$  is shown in Fig. 2(a). For small strain rates, both inertia and deformation of the particles are negligible, and the stress grows with strain rate as  $\sigma = \eta \dot{\gamma}^\nu$ , characteristic for a power-law fluid. The “effective viscosity”  $\eta(\phi)$  is measured in this regime and is a function of the volume fraction, as shown in Fig. 1 for the Newtonian case ( $\nu = 1$ ). At larger strain rates and in weakly damped systems ( $\zeta = 0.001$  or  $\nu > 1$ ), one observes a shear thickening regime, which can be ascribed to inertia. Conversely, for stronger damping ( $\zeta = 0.1$  and  $\nu < 1$ ) and, in particular, for volume fractions close to  $\phi_c$  [23], one observes a shear-thinning regime, when particle deformation starts to be relevant.

Quasistatic simulations consist of successively applying small steps of shear and minimizing the total potential energy. By construction, they generate particle trajectories at  $\dot{\gamma} \rightarrow 0$ . An elementary strain step of  $\gamma_0 = 5 \times 10^{-5}$  is used. After each change in boundary conditions, the particles are moved affinely to define the starting configuration for the minimization, which is performed using conjugate gradient techniques [24]. The minimization is stopped when the nearest energy minimum is found. As no static, force-balanced state exists below the jamming point ( $\phi < \phi_c$ ), the interparticle forces at the minimum are strictly zero; i.e., the particles can always arrange in such a way as to avoid mutual overlaps. Thus, each minimized configuration corresponds to a true hard-sphere state, and the resulting particle trajectories can be viewed as a sequence of snapshots of a flowing hard-sphere system at zero temperature. Particle motion in such a system is driven by steric exclusion and the lack of free volume. In particular, particles have to move over larger distances when the jamming point is approached, to find a new overlap-free state compatible with the imposed shear [25].

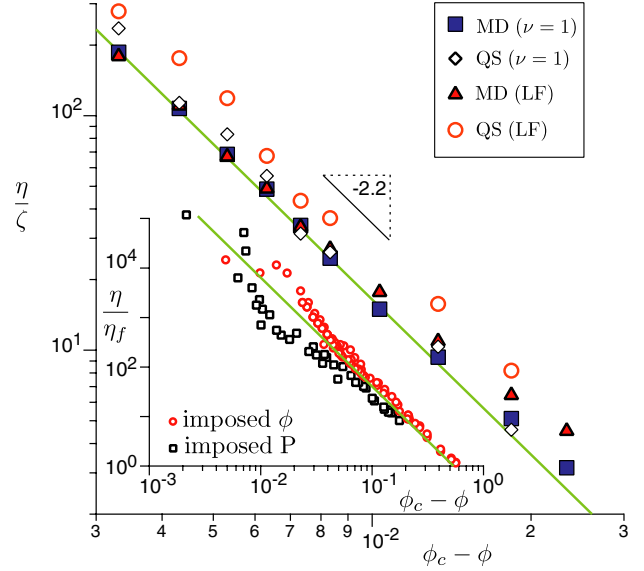


FIG. 1 (color online). Viscosity  $\eta$  normalized by the friction coefficient  $\zeta$  as a function of the volume fraction  $\phi$ , measured from molecular dynamic (MD) and QS simulations, for a dissipation induced by viscous drag forces of Eq. (1) (labelled  $\nu = 1$ ) or the lubrication-like mechanism of Eq. (3) (labelled LF). In MD, the viscosity is measured in the low shear rate regime for  $\dot{\gamma} = 10^{-6}$  and  $\zeta = 10^{-1}$ . In this regime,  $\eta/\zeta$  does not depend on the precise value of these parameters, as shown in Fig. 2(a). The quantitative agreement between MD ( $\nu = 1$ ) and MD (LF) is coincidental. Inset: compilation of experimental data available in the literature at imposed pressure  $P$  (with  $\phi_c = 0.587$ ) and imposed volume fraction  $\phi$  (with  $\phi_c = 0.615$ ) for the ratio of suspension to solvent viscosity.

Without particle overlaps, all the contact forces and therefore the shear stress are strictly zero in the QS simulation. Still, an effective shear stress and viscosity can be obtained from the power  $\Gamma$  per unit surface that would be dissipated along the QS trajectories, if the dissipation mechanism of Eq. (1) was present.  $\Gamma$  is equal to the power injected per unit volume in the system,  $\sigma \dot{\gamma}$ , and can be expressed as

$$\Gamma = L^{-2} \left\langle \sum_i \vec{F}_i^{\text{visc}}(\vec{v}_{i,\text{qs}}) \cdot [\vec{v}_{i,\text{qs}} - \vec{v}_{\text{flow}}(\vec{r}_i)] \right\rangle \quad (2)$$

From this expression, we deduce the viscosity:

$$\eta = \frac{\Gamma}{\dot{\gamma}^{1+\nu}} = -\zeta \frac{N}{L^2} \frac{\langle \delta v^{1+\nu} \rangle}{\dot{\gamma}^{1+\nu}} = -\zeta \frac{N}{L^2} \int \Delta^{1+\nu} P(\Delta) d\Delta. \quad (3)$$

where  $P(\Delta)$  is the probability distribution function (PDF) of the particle velocity rescaled by the shear rate  $\Delta = \delta v / \dot{\gamma}$ . As particle coordinates in the QS simulation are only available at discrete steps, one has to define an effective particle velocity  $\vec{v}_{\text{qs}} = \dot{\gamma} \delta \vec{r} / \gamma_0$  from the particle displacement  $\delta \vec{r}$  during such a single step. Therefore,  $\Delta$  is also the displacement rescaled by the strain interval  $\gamma$  and

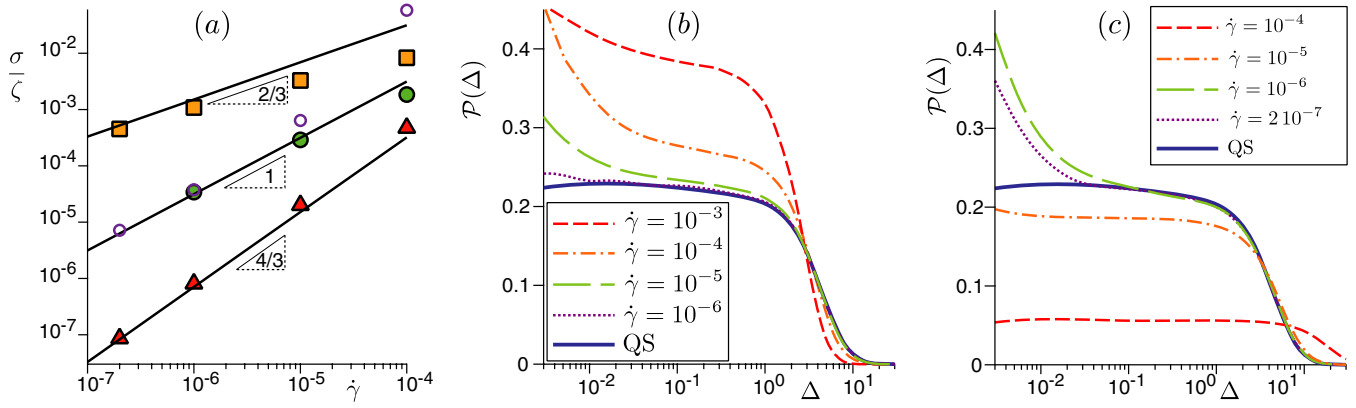


FIG. 2 (color online). Rheology and velocity fluctuations at  $\phi = 0.836$ . (a) Relation between stress  $\sigma$  and strain rate  $\dot{\gamma}$  obtained from MD simulations for  $\zeta = 10^{-1}$  at  $\nu = 2/3$  (■),  $\nu = 1$  (●), and  $\nu = 4/3$  (▲) and for  $\zeta = 10^{-3}$  at  $\nu = 1$  (○). A small strainrate regime can be identified where  $\sigma = \eta \dot{\gamma}^\nu$ . The solid lines correspond to this expression, with  $\eta$  independently determined from the QS simulation using Eq. (2). (b–c) PDF  $P(\Delta)$  of the rescaled velocity fluctuations  $\Delta = \delta v / \dot{\gamma}$  at  $\nu = 1$ , for (b)  $\zeta = 10^{-1}$  and (c)  $\zeta = 10^{-3}$ .

$P(\Delta)$  the van Hove function. Note that viscosity is related to the  $(\nu + 1)$ st moment of the velocity fluctuations, and thus of  $P(\Delta)$  [Eq. (2)].

**Results.**—To statistically characterize the trajectories, we consider the probability distribution for particle velocities,  $P(\Delta)$ . We concentrate on the velocity component in the gradient direction (y component), which automatically eliminates trivial particle motion due to the average flow field. When the strain rate is small enough,  $P(\Delta)$  reaches a limiting form [dotted line in Figs. 2(b) and 2(c)], which is directly related to the small strainrate power-law regime of Fig. 2(a). Whenever the rheology  $\sigma(\dot{\gamma})$  deviates from this asymptotic behavior, the distribution function  $P(\Delta)$  deviates from its asymptotic form as well. Interestingly, the approach toward this asymptotic form is rather different in the weakly damped, i.e., shear thickening, system [Fig. 2(b) and ● in Fig. 2(a)] as compared to the strongly damped, shear-thinning system [Fig. 2(c) and ○ in Fig. 2(a)].

The velocity fluctuation PDFs obtained in the QS simulation [solid lines in Figs. 2(b) and 2(c)] are similar to those obtained in MD in the limit of vanishing  $\dot{\gamma}$ . In particular, the sharp shoulder at  $\Delta \approx 4$  is well reproduced for both strongly ( $\zeta = 10^{-1}$ ) and weakly ( $\zeta = 10^{-3}$ ) damped systems. Furthermore, as shown in Fig. 3, the small strainrate form of  $P(\Delta)$  only weakly depends on the value of the exponent  $\nu$ . Again, the most pronounced feature is the shoulder, which is nearly identical in all four simulations. However, small differences between MD and QS still remain, especially for small damping [Fig. 2(c)] or  $\nu > 1$  (Fig. 3). Here, a rise at small  $\Delta \rightarrow 0$  is observed at the smallest strain rates, which is not present in the QS simulation. Importantly, such small velocities do not contribute to the second moment of the distribution and therefore are irrelevant for the dissipated energy and the viscosity [Eq. (2)]. By way of contrast, these small differences may be important for the number of interparticle contacts. As it turns out, the coordination number  $Z$ , which is the

number of contacts per particle (taken from simulation snapshots), strongly varies with either  $\nu$  or  $\zeta$  and is also different in the QS simulation; its value changes from  $Z_{\text{iso}} \approx 4$ , i.e., close to the isostatic state, down to small values  $Z < 1$ .

We conclude that the overall features of the particle trajectories in the MD simulations are statistically comparable to those in the QS simulation. The small strainrate power-law fluid regime (Newtonian for  $\nu = 1$ ) should therefore be considered as a true QS limit, which is by no means obvious. In fact, the QS limit seems much better defined here ( $\phi < \phi_c$ ) than in the plastic flow regime ( $\phi > \phi_c$ ), where QS simulations have usually been

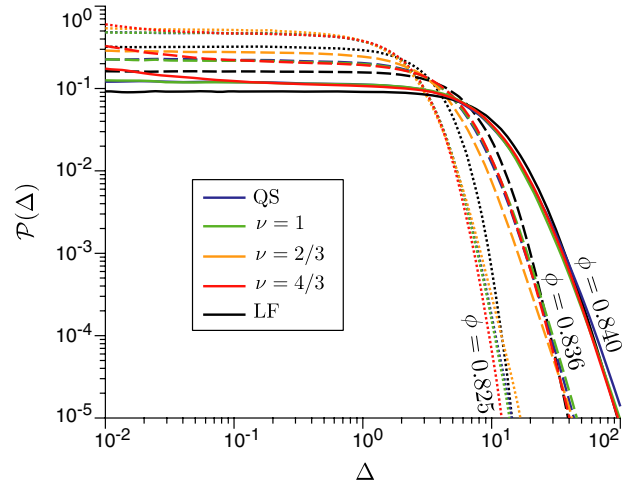


FIG. 3 (color online). Comparison of the PDF  $P(\Delta)$  of the rescaled velocity fluctuations  $\Delta = (v - v_{\text{flow}}) / \dot{\gamma}$  obtained for the different computational models at different volume fractions  $\phi$ . Measurements are performed in the low shear rate asymptotic regime for  $\dot{\gamma} = 10^{-6}$  and  $\zeta = 0.1$ . The three values of  $\nu$  correspond to the dissipation mechanism of Eq. (1), the LF label refers to the lubrication-like mechanism of Eq. (3), and QS to quasistatic simulations.

applied, but where they suffer from a dependence on system size [8,14].

One important consequence of the equivalence MD-QS is that one set of QS trajectories can be used to determine the flow rheology for different values of  $\nu$ . Figure 2(a) compares the rheology obtained using MD (data points) and QS (solid line) simulations. They nicely collapse on each other when MD simulations are considered in the limit of small shear rate. Figure 1 shows the viscosity  $\eta$  determined from both simulations as a function of volume fraction  $\phi$ . Beyond noting the quality of the collapse, one observes that the viscosity diverges with  $\phi_c - \phi$ , with a scaling exponent  $\approx 2.2$ , consistent with the values measured experimentally.

Equation (2), giving the power dissipated per unit volume, leads to the scaling law  $\eta \sim \langle \delta v^{1+\nu} \rangle$ , which connects the divergence of the macroscopic viscosity to the scaling law followed by the microscopic particle motion  $\delta v \sim (\phi_c - \phi)^{-\beta}$ . Thus, the seemingly harmless power balance turns into a relation between the exponents controlling the divergence of velocity fluctuations and that of viscosity:  $\alpha = \beta(1 + \nu)$ . We have recently shown that  $\beta \approx 1.1$  [25], which gives (for  $\nu = 1$ )  $\alpha \approx 2.2$ , consistent with the exponent extracted from the MD data in Fig. 1. Note however, that subdominant corrections can lead to apparent exponents that, in the considered range of densities, may not reflect true asymptotic behavior [19,26].

*Discussion.*—The small strainrate rheology,  $\sigma = \eta \dot{\gamma}^\nu$ , as well as the divergence of the viscosity,  $\eta \sim \delta \phi^{\beta(1+\nu)}$ , depend on the value of  $\nu$ . On the other hand, the underlying particle trajectories are hardly affected by changing  $\nu$ . This points to a certain decoupling between particle trajectories and the dissipative process. In this picture, the statistical properties of trajectories are largely governed by the structural singularity of random close packing and the lack of space available for particle motion. On the other hand, system-specific dissipation mechanisms affect the rheological properties via the dissipated energy along these geometrically predetermined trajectories. Certainly, such a decoupling cannot be realized in a perfect manner, as shown by the small differences of  $P(\Delta)$  at small  $\Delta$  and in the tails (Figs. 2 and 3). Nevertheless, it seems to be strong enough so that the various flow curves [Fig. 2(a)] and the viscosity (Fig. 1) can accurately be predicted from the sole knowledge of one set of QS trajectories. The scaling law relating the viscosity to the volume fraction is a directly testable prediction of the central idea of this Letter. It proposes to measure the rheology of particles suspended in a nonNewtonian solvent like a polymer melt or a viscoplastic fluid.

In order to investigate the universality of the decoupling phenomenon, we have conducted additional simulations with a damping that describes a modified lubrication force [27] between neighboring particles  $i$  and  $j$ :

$$\vec{F}^{\text{diss}}(\vec{v}_i, \vec{v}_j) = -\zeta \hat{n}_{ij} [\hat{n}_{ij} \cdot (\vec{v}_i - \vec{v}_j)], \quad (4)$$

In agreement with previous (overdamped) simulations [9,23], the spatial velocity-correlation function is qualitatively different in the models of Eqs. (1) and (3) (not shown). Still, the probability distribution  $P(\Delta)$  (Fig. 3) is remarkably similar across all models considered. In particular, the scale of velocity fluctuations increases on approaching the critical volume-fraction  $\phi_c$ , and the overall agreement between the different curves seems to improve. This supports our interpretation of the role of close packing for the particle trajectories. Furthermore, starting with the QS trajectories, a calculation similar to Eq. (2) can again be used to predict the viscosity. As Fig. 1 illustrates (open circles), this calculation is quite accurate but slightly overestimates the true viscosity (triangles), roughly by a factor  $\approx 1.5$ .

In conclusion, singular velocity fluctuations cause a dynamical contribution to the divergence of the viscosity, as independently noted in Ref. [18]. These velocity fluctuations are surprisingly conserved across different computational models, which we explain with geometric features and the lack of available space close to the jamming transition. Our results complement those obtained in Ref. [18], for frictionless hard-spheres. In that system, the jamming transition coincides with the isostatic threshold and the flow properties can be related to the geometry of the contact network. The coordination number  $Z$  is then the relevant control parameter. Our results bridge the gap between such an ideal system and those where inertia and elasticity lead, for a given volume fraction  $\phi$ , to strong changes of  $Z$ . Indeed, in our simulations, the value of  $Z$  has no immediate predictability and  $\phi$  is the only relevant parameter. Our results open the promising perspective of the existence of an inherent contact network that would govern the topography of the energy landscape. Such a concept would establish the missing connection between volume fraction and connectivity.

B. A. and J. L. B. are supported by Institut Universitaire de France; C.H. is supported by the Deutsche Forschungsgemeinschaft, Emmy Noether program: No He 6322/1-1; J. L. B. acknowledges a useful discussion with A. Lemaître.

- 
- [1] F. Bolton and D. Weaire, *Phys. Rev. Lett.* **65**, 3449 (1990).
  - [2] M. Clusel, E. I. Corwin, A. O. N. Siemen, and J. Brujic, *Nature (London)* **460**, 611 (2009).
  - [3] F. Boyer, E. Guazzelli, and O. Pouliquen, *Phys. Rev. Lett.* **107**, 188301 (2011).
  - [4] M. van Hecke, *J. Phys. Condens. Matter* **22**, 033101 (2010).
  - [5] H. A. Makse, N. Gland, D. L. Johnson, and L. M. Schwartz, *Phys. Rev. Lett.* **83**, 5070 (1999); H. A. Makse, N. Gland, D. L. Johnson, and L. M. Schwartz, *Phys. Rev. E* **70**, 061302 (2004).

- [6] M. Wyart, *Ann. Phys. (Paris)* **30**, 1 (2005).
- [7] P. Sollich, F. Lequeux, P. Hébraud, and M. E. Cates, *Phys. Rev. Lett.* **78**, 2020 (1997); P. Hébraud and F. Lequeux, *Phys. Rev. Lett.* **81**, 2934 (1998).
- [8] A. Lemaître and C. Caroli, *Phys. Rev. Lett.* **103**, 065501 (2009).
- [9] B.P. Tighe, E. Woldhuis, J.J.C. Remmers, W. van Saarloos, and M. van Hecke, *Phys. Rev. Lett.* **105**, 088303 (2010).
- [10] D.L. Malandro and D.J. Lacks, *J. Chem. Phys.* **110**, 4593 (1999).
- [11] C.E. Maloney and A. Lemaître, *Phys. Rev. E* **74**, 016118 (2006).
- [12] A. Tanguy, F. Leonforte, and J-L. Barrat, *Eur. Phys. J. E* **20**, 355 (2006).
- [13] C. Heussinger and J.-L. Barrat, *Phys. Rev. Lett.* **102**, 218303 (2009).
- [14] C. Heussinger, P. Chaudhuri, and J.-L. Barrat, *Soft Matter* **6**, 3050 (2010).
- [15] A. Ikeda, L. Berthier, and P. Sollich, *Phys. Rev. Lett.* **109**, 018301 (2012).
- [16] C. Bonnoit, T. Darnige, E. Clement, and A. Lindner, *J. Rheol.* **54**, 65 (2010).
- [17] P. Mills and P. Snabre, *Eur. Phys. J. E* **30**, 309 (2009).
- [18] E. Lerner, G. Düring, and M. Wyart, *Proc. Natl. Acad. Sci. U.S.A.* **109**, 4798 (2012).
- [19] D. Vågberg, D. Valdez-Balderas, M. A. Moore, P. Olsson, and S. Teitel, *Phys. Rev. E* **83**, 030303 (2011).
- [20] D.J. Durian, *Phys. Rev. Lett.* **75**, 4780 (1995).
- [21] A. Scala, T. Voigtmann, and C. D. Michele, *J. Chem. Phys.* **126**, 134109 (2007).
- [22] B. Lander, U. Seifert, and T. Speck, *Europhys. Lett.* **92**, 58001 (2010).
- [23] P. Olsson and S. Teitel, *Phys. Rev. Lett.* **99**, 178001 (2007).
- [24] S.J. Plimpton, *J. Comput. Phys.*, **117**, 1 (1995); <http://lammps.sandia.gov/index.html>.
- [25] C. Heussinger, L. Berthier, and J-L. Barrat, *Europhys. Lett.* **90**, 20005 (2010).
- [26] P. Olsson and S. Teitel, *Phys. Rev. E* **83**, 030302 (2011).
- [27] In order to ensure Newtonian flow at small strain rates, we choose an interaction range  $r_c^{\text{diss}} = 1.5(r_i + r_j)$  that is larger than the range for elastic interactions. In effect, this corresponds to a lubrication force with a divergence that is cut off at short distances.